UNIVERSITY OF CALIFORNIA

Santa Barbara

Late Pleistocene to Holocene environmental history of Devereux Slough

A Thesis submitted in partial satisfaction of the

requirements for the degree Master of Science

in Earth Science

by

Zachary Nelson

Committee in charge:

Professor Alex Simms, Chair

Professor Lorraine Lisiecki

Professor Edward A. Keller

January 2018

The thesis of Zachary Nelson is approved.

_____
Edward A. Keller

_____
Lorraine Lisiecki

_____
Alexander Simms, Committee Chair

January 2018

Late Pleistocene to Holocene environmental history of Devereux Slough

2018

by

Zachary Nelson

ACKNOWLEDGEMENTS

Thank you to Alex Simms for conceiving this Master's project and introducing me to the many intricacies of coastal sedimentology. Thanks to the Earth Research Institute for a summer fellowship in 2017. Many thanks to Laura Reynolds, Elisabeth Steel, Julie Zurbuchen, Michael Bentz, Dillon Osleger and Michael Troung for help with fieldwork, lab procedures and thesis writing guidance.

We would also like to thank Cristina Sandoval and Lisa Stratton at the Coal Oil Point Reserve and Cheadle Center for Biodiversity and Ecological Restoration (CCBER) for helping facilitate gaining access to my study site. Additional financial support was provided by the Southern California Earthquake Center and the Santa Barbara Coastal LTER. The Southern California Earthquake Center is funded by the National Science Foundation Cooperative Agreement EAR-1033462 and the United States Geological Society Cooperative Agreement G12AC20038. Any opinions, findings, and conclusions or recommendations expressed in this material are those of the author(s) and do not necessarily reflect the views of the National Science Foundation or the United States Geological Society.

ABSTRACT

Late Pleistocene to Holocene environmental history of Devereux Slough

by

Zachary Nelson

Environmental histories of coastal regions are important for providing historical perspectives on restoration projects as well as evaluating the risks due to tsunami and other coastal hazards. Currently, little is known about the Late Pleistocene through Holocene tsunami history of the highly populated Southern California coast. Devereux Slough is a flooded stream valley near the Southern Californian city of Santa Barbara. In this study I analyze six new cores from Devereux Slough containing sediments spanning the last 16 ka in order to provide insights into past coastal hazards and environmental conditions of the estuary. Five facies representing four main environments are identified. These facies include a pebbly sandy mud, a bioturbated mud, a laminated silt, a well sorted sand, and a brown silt. The succession of environments represented by these facies largely reflects the late Pleistocene/Holocene transgression following the last glacial maximum ~20 ka. The laminated silt resembles deposits from modern alluvial fans feeding the slough from gullies on its margins. The temporal distribution of this facies reflects that of floods preserved in marine cores from the Santa Barbara Basin and likely records periods of terrestrial flooding across the landscape. Interbedded well-sorted sand and laminated mud date to 3930±410 cal BP and likely represents alternating storm overwash and terrestrial floods. No evidence of

marine inundation at the time of proposed large earthquakes on the nearby Pitas Point Thrust were found suggesting that either the fault was not tsunamigenic, the tsunami produced was less than 2 m in elevation, or the tsunami was confined to the eastern-most portions of the Santa Barbara Channel. Two sea-level index points based on radiocarbon ages from the intertidal gastropod *Cerithidea californica* provide rates of vertical motion for two locations within the slough. One index point suggests uplift at a rate of 0.25±0.39 mm/yr and the second subsidence at a rate of 0.05±0.39. As both are within error of zero and I have not accounted for compaction, the slough is likely on the uplifting side of the Moore Ranch Fault placing the fault to the north of the slough.

TABLE OF CONTENTS

LIST OF TABLES AND FIGURES

Introduction

Due to their high preservation potential, estuarine sediments within flooded stream valleys often contain a near continuous record of environmental changes (Belknap and Kraft, 1985; Simkins et al., 2012; Elliot et al., 2015). An understanding of past environmental changes within estuaries provides insight into possible future hazards and how estuaries respond to environmental changes. Along the California coast these important hazards and environmental changes include storms, tsunamis, subsidence, sea-level rise, earthquakes and strong El Niño winters. However, despite its high population density, little is known about the environmental history of the tectonically active California coast estuaries. One of these pressing hazards is the uncertainty surrounding the magnitude and tsunamigenic potential of earthquakes along faults in the Santa Barbara Channel, which could expose the 200,000+ people living in the area to unforeseen threats. Devereux Slough is also the site of a large restoration project and this study provides a historical perspective of what the estuary looked like before recent anthropogenic changes.

The purpose of this thesis is to address four specific questions related to the environmental history and coastal hazards of Devereux Slough and the Santa Barbara Channel Coast. First, did the proposed large earthquakes along the Pitas Point Fault – Ventura Avenue Anticline along the eastern Santa Barbara Channel (Rockwell et al., 2016) produce large tsunami as suggested by numerical models (e.g. Ryan et al., 2015)? Second, what is the record of other overwash events (such as storms) along the Santa Barbara Channel? Third, what is the subsidence and/or relative sea-level history of Devereux Slough and what might tell us about the history and/or location of faults near the slough? Fourth, what is the record of terrestrial runoff within Devereux Slough and how does it relate to

other regional records of precipitation and fluvial flooding (e.g. Kriby er al., 2012; Du et al., 2017)?

To answer these questions concerning what impact storms, tsunamis, subsidence, sea-level rise, earthquakes and El Niño winter storms have on the local population and to gain comprehensive insight into the depositional history of the region, I examined six cores collected within the slough. Through a detailed analysis of these cores I provide valuable insight into the depositional history of the slough including the occurrence of (or absence of evidence for) past storms, flooding, and tsunami.

Background

Geologic Framework

Devereux Slough is located in the flooded river valley of Devereux Creek along the northern Santa Barbara Channel of Southern California. Devereux Creek is a small creek draining an area of 9.6 km^2 and not connecting to the watersheds draining the Santa Ynez Mountains to the north (Figs. 1 and 2). The creek valley is incised into a marine isotope stage 3 marine terrace whose deposits are exposed in the 12-20 m high bluffs that line much of the UCSB coastline (Gurrola et al., 2014). Late Pleistocene and Holocene rising sea levels flooded the river valley producing the current lagoon. Tides along the northern Santa Barbara Channel coastline are microtidal with a mean diurnal tidal range of 1.65 m (www.tidesandcurrents.noaa.gov; last accessed 8/2/17).

Southern California is a tectonically active region. Although large scale features such as the San Andreas Fault are well documented, other smaller systems such as the Pitas Point, Oak Ridge, and Red Mountain faults are only recently receiving international

attention and their subsurface geometries are still a matter of debate (Marshall et al., 2013; Marshall et al., 2017; Hubbard et al., 2014; McAuliffe et al., 2015; Rockwell et al., 2016; Johnson et al., 2017; Rockwell et al., 1988). The Santa Ynez Mountains and these north-dipping thrust faults are part of the larger Santa Barbara Fold Belt (Gurrola et al., 2014). A detailed understanding of the subsurface fault geometries is important for determining the potential risk these faults have on the densely populated urban areas of Southern California (Marshall et al 2017). Coastal uplift during large magnitude (M >7.0) earthquakes along the Pitas-Point Thrust – Ventura Avenue Anticline created Holocene marine terraces along the northern Santa Barbara Channel. These earthquakes are thought to have possibly occurred at 955 BP, 2090 BP, 4400 BP and 6670 BP (Hubbard et al., 2014; McAuliffe et al., 2015; Rockwell et al., 2016). They may have also produced tsunami (Ryan et al., 2015) but evidence for tsunami deposits within the Santa Barbara Channel have yet to be identified.

In addition to the Pitas-Point Thrust – Ventura Avenue Anticline, other smaller local structures are found in the area. Dibblee (1966), Minor et al. (2009) and Gurrola et al (2014) mapped many west and northwest striking oblique reverse faults and north east striking lateral tear faults within the Santa Barbara Region. These faults include the Dos Pueblos Fault, Carneros Fault, San Jose Fault, San Pedro Fault, and the More Ranch Branch of the Mission Ridge Fault system (Gurrola et al 2014)(Fig. 1). The location of the More Ranch Branch in the vicinity of Devereux Slough is uncertain and a consensus has yet to be reached concerning which section(s) of the branch is (are) active (UCSB Environmental Impact Report; Gurrola et al., 2014).

Late Pleistocene and Holocene Sea-Level Changes

Across much of the globe, sea levels have generally risen over the last 20 ka (Fairbanks 1989; Bard et al 1996). However, the details of how sea level has risen vary from region to region due to glacial isostatic adjustment, steric affects, and local vertical movements. Reynolds and Simms (2015) produced a local relative sea-level curve for southern California based on tectonically-corrected estuarine sea-level indicators. They show that from the end of the last glacial maximum until about 4 ka sea level rose at rates >5 mm/year; while in the past 4 ka, the rate slowed to 0.8 mm/year. This sea-level record provides an excellent datum for the calculation of local fault motions and regional patterns of uplift or subsidence (Simms et al, 2016).

Climate

Santa Barbara has a Mediterranean climate with annual winter rains and dry summers (Kirby et al 2007). The climate over the past 10 ka has varied from a wetter fluvial period from the early Holocene until 8 ka, when climate shifted to a drying trend that has persisted to present day (Kirby et al 2007, 2010). Higher resolution climatic records of the past 3 ka show that winter storms are the main controllers of energy input to a system and contribute heavily to the amount of rainfall (Kirby et al 2014). Southern California experienced dry conditions during the Late Holocene Dry Period between 2500 and 2000 Years BP (Kirby et al 2014) and over the past 1 ka alternating periods of “Epic Droughts” at 762, 865, 981, 1079 cal BP and large-magnitude floods at 100, 186, 402 and 694 cal PB (Kirby et al 2014, Cook et al 2004). Recent work documenting flood deposits within the varved deep-marine sediments of the Santa Barbara Basin provide an excellent record of

past flooding of the rivers and streams entering the Santa Barbara Channel (Du et al., 2017). Based on this work, periods of frequent flooding occurred at 0.9 ka to 2.8 ka , 4.7 ka to 5.2 ka, 6.4 ka to 6.6 ka, 7.2 ka to 7.6 ka and 7.8 ka to 8.6 ka.

Methods

Six cores were collected from Devereux Slough using two coring techniques (Figure 2). Three longer length cores ranging from 5 m to 18 m were collected using a GeoProbe 7822DT within the former Ocean Meadows Golf Course before ongoing restoration started; the diameter of these cores is 4 cm and they were collected in 1.5 m intervals. Shorter cores of less than 3 m in length and a diameter of 7.6 cm were collected from a raft using a vibracoring system in the flooded portions of the lagoon. Core locations were determined using a TopCon Hyperlite+GPS. Elevations were corrected to NAVD88 (North American Vertical Datum of 1988) using the online NOAA OPUS site www.ngs.noaa.gov/OPUS/; last accessed December, 2017) (Simms et al 2016). Physical descriptions of the cores include color, texture, the presence of sedimentary structures, any bedding planes observed, macro- and micro-fauna, bioturbation and the presence of plant or organic material. The sedimentary environments are based on interpretations from the physical observations and faunal similarity to modern environments.

Magnetic susceptibility was determined by extracting samples at 2.5 cm intervals and placing each in 8 cm^3 plastic cubes. Mass magnetic susceptibility was measured twice on each sample, with the y-axis rotated 180 degrees per analysis. All samples were analyzed using a Bartington MS2 Magnetic Susceptibility Instrument at 0.465 kHz. Measurements

were made to the 0.1 decimal place and reported as mass magnetic susceptibility in SI units ($x10^{-7}$ m^3 kg^{-1}) (Kirby et al 2007).

Radiocarbon ages were obtained from two gastropod *Cerithidea californica*, and eighteen charcoal fragments within the cores. The two shells analyzed were in pristine condition and were not worn, bleached or chipped. The charcoal picked was preferentially selected for larger particles (>1 mm) to reduce the possibility of sample contamination. If charcoal pieces were too small (< 1 mm) to make a sufficient sample weight individually, more samples were chosen from the same horizon to obtain a sufficient sample weight. The two *C. californica* samples were calibrated using Calib 7.1 (Reimer et al 2013) with the ^{14}C radiocarbon reservoir delta R value of 171 ± 154 years based on the work of Holmquest et al (2015). We used the Southern California estuary reservoir of 217±129 years for the bivalve samples (Holmquest et al., 2015). Once calibrated, Bchron (Haslett and Parnell 2008) was used to create an age to depth correlation for each core.

Samples were analyzed for grain size every 5 cm (every other magnetic susceptibility sample) using a CILAS 1190 particle size analyzer capable of measuring grains within the 0.04 um to 2500 um range. Grain size was determined by first pre-treating the sample with 30-50 ml of 30% H_2O_2 to remove organic matter, followed by a DI water boil, following the protocols described by Kirby et al (2014).

Ostracods were identified in cores using a 63 μm sieve and DI water to isolate the shells and sand particles. Family to Subfamily identifications in the Podocopida Order and habitat conditions were provided by Dr. Finn Viehberg of the University of Cologne. Family abundances were counted through cores UDX 15-01 and DX 11-04 every 5 cm to determine

any change in subfamily dominance. These cores were chosen due to their location and length.

Results

Six cores were obtained reaching depths of 18 m (Fig. 3). The longest core, UDX 15-01 was obtained from the center of the former golf course, which was previously the center of the slough. The cores all contain similar sediments, generally alternating blue-green muds underlain by sandy silt deposits and interrupted by sand beds with increasing frequency closer to the shore. I identified five facies based on physical characteristics observed in the cores and grain size (Figure 4). These facies include a Pebbly Sandy Mud, Laminated Silt, Bioturbated Mud, Well Sorted Sand and Brown Silt facies.

The Pebbly Sandy Mud (Fig. 5A) is characterized by a poorly sorted mix of pebbles, sand, silt and clay. No observable bedding, lamination, or sedimentary structures are apparent. The magnetic susceptibility of this facies has the largest average of 3.8 $x10^{-7}$ m^3 kg^{-1}, and most varied with peaks up to 25 $x10^{-7}$ m^3 kg^{-1} mass magnetic susceptibility. The pebbles and sand are angular to sub angular, and represent a mixture of rock types and minerals.

The Laminated Silt facies (Fig. 5B) contains on average 66% silt, 28% clay with 6% sand, and is interbedded with brown to tan silty laminations. Little variability in magnetic susceptibility (average 1.23 $x10^{-7}$ m^3 kg^{-1}) and grain-size is observed in this facies (Fig. 6). Some of the laminations are composed of coarse silt or very fine sand (Fig. 5B). The sand component is dominantly sub angular quartz with a few feldspar grains.

The Bioturbated Mud facies (Fig. 5D) has a similar grain size as the laminated silt facies; 65% silt, 34% clay with 1% sand, and also has little variation in magnetic susceptibility (average 0.68 x10^{-7} m^3 kg^{-1}) and grain-size characteristics. The major difference is the absence of laminations, the lower percentage of sand, and the presence of mottling. Sieved sediment samples also contain sub angular grains mostly consisting of quartz sand with few feldspar grains.

The Well Sorted Sand facies (Fig. 5C) consists of a well sorted clean sand comprised of 90% quartz, 6% feldspars and 4% lithics. No laminations, bedding or sedimentary structures were observed in the core. Little variability in magnetic susceptibility (average 0.68 x10^{-7} m^3 kg^{-1}) and grain-size occur (Fig. 6), similar to the bioturbated mud and laminated silt facies. The medium sands have an average grain-size of 0.35 mm.

The Brown Silt facies (Fig. 5D) is composed on average of 16% sand, 66% silt and 18% clay. A distinct color change occurs at the contact of this facies with the overlying bioturbated mud facies (Fig. 6). The transition is capped by a bed of darker color driven by a higher organic content. This darker bed has a sharp or erosional top with a gradational base and may represent a weakly-developed A-horizon (Fig. 5D). Both magnetic susceptibility (0.5-10 x10^{-7} m^3 kg^{-1}) and grain-size (±20%) varies widely in this facies.

Seven modern beach and dune sand samples were also characterized in order to provide analogues for interpreting the sand facies observed in the cores. Sand from the modern beach at Coal Oil Point Beach and active dunes behind the beach have median grain sizes of 0.35 mm and 0.40 mm respectively. The beach has average Quartz, Feldspar and Lithic (QFL) distributions of 73,17,10 and the dunes are represented by average QFL distributions of 75,17,8.

Ostracods were identified and counted at 5 cm intervals within cores DX 11-04 and UDX 15-01. Only two samples with ostracods were found below 600 cm; all other occurrences of ostracods are found above this depth. Three main Families of ostracods were found in the cores and include Limnocytheridae, which thrives in a fresh to brackish environment, Cyprideis, which lives in brackish to lagoon environments, and the halo-tolerant Sarscypridopsis, which inhabit saltwater marsh environments. One additional family, Llyocypris, of which only five specimens are found, were identified. These are thought to have washed in from fresh-water environments upstream of the slough. The abundance of families transitions at a depth of 330 cm in core UDX15-01 and 350 cm in core DX11-04 (Figs. 6 and 7). At this transition, the abundance of specimens from the respective families shifts from being dominated by Limnocytheridae or Cyprideis to Sarscypridopsis. At depths of 350 and 330 cm in cores UDX15-01 and DX11-04, Sarscypridopsis composes nearly 50% of the sample populations (Figs. 6 and 7). This dominance of Sarscypridopsis decreases to zero occurrences at 50 cm with no Sarscypridopsis occurring above that depth and the surface (Figs. 6 and 7)

Twenty-one radiocarbon ages were collected from the cores (Table 1) and compiled using Bchron to produce an age model for each core (Figure 8). Bchron plots approximate an age range for sediment at every depth between the measured ages in each core. The longest core, UDX 15-01, contains the most detailed chronology with eleven ages, while the remaining ages were obtained from cores UDX15-02, DX11-03 and DX11-04. The oldest age was obtained from core UDX15-01. It dated to 18,490 cal BP and was found within the Brown Silt facies at a depth of 1721 cm. An average sedimentation rate of 1 mm/yr was

found in core UDX15-01 (Figure 8). The rates from other cores are 1mm/yr in core UDX 15-02, 1.45 mm/yr in core DX 11-04 and 0.75 mm/yr in core DX 11-03 (Figure 8).

Discussion

Facies Interpretation

Based predominately on its current location as well as the poorly sorted mix of pebbles, sand, silt, and clay, the lack of bedding, laminations or sedimentary structures, and the highly variable magnetic susceptibility, the Pebbly Sandy Mud is interpreted to represent the material added to construct the Ocean Meadows Golf Course in 1966. It represents the anthropogenic filling of the slough.

Based on the finer grain-sizes, bioturbation, and presence of a mix of salt tolerant, marsh, and brackish ostracods as well as the intertidal gastropod *Cerithidea californica*, the bioturbated muds are interpreted to represent deposition within a shallow, quiet-water, marine-influenced backbarrier-type environment – either a lagoon or shallow coastal lake with an occasional connection with the ocean. The environment was probably very similar to what the slough looks like today when filled with water. The near absence (a total of 5 were found in all the samples used to count ostracods) of foraminifera suggests the slough lacked consistent tidal flushing.

The Laminated Silt facies is found today in the top of core DX11-03, which was collected near a historically formed minor alluvial fan/fan delta created after disturbance to the landscape when building the road separating the upper and lower reaches of Devereux Slough. Based largely on this spatial correlation, the laminated silt facies is interpreted to represent small alluvial fans/fan deltas prograding into the lagoon from its margins (Figure

9). The laminated silt facies has a higher sand content (6%) than the bioturbated mud facies (1%), as would be expected in a fluvial-feed deposit. The sands are finer (0.1 mm) than the beach sands (0.35 mm) suggesting a source other than the marine realm. The scarcity of ostracods in their deposits also points to a more fluvially-influenced environment. However, the presence of a stray *C. californica* suggests the features are low-relief and never built that high above the lagoon surface. Intervals of the laminated silt facies can be correlated along dip throughout the entire length of the lagoon (Fig. 10). Thus, the alluvial fans/fan deltas likely represent deposition feed from gullies or sheetwash entering the system rather than a larger axial system prograding down the axis of the slough. If the later, we would expect a facies transition from the laminated silts to the bioturbated muds at some point down the axis of the system.

Based on the grain-size, sorting, and mineralogical similarity to modern beach deposits, the well-sorted sand facies is interpreted to represent washover deposits. Its increasingly common occurrence in the more seaward reaches of the lagoon and absence in the more landward reaches of the lagoon support this interpretation.

Based on the absence of fauna, brown color, variable magnetic susceptibility and a possible soil horizon development, the Brown Silt facies is interpreted to represent a fluvial/alluvial floodplain. Its uninterrupted thickness at the base of cores UDX15-01 and UDX15-02 suggest it formed before initial flooding of the stream valley to form a lagoon. A comparison between its age and depth and that of a regional sea-level curve (Reynolds and Simms, 2015) supports this interpretation.

Stratigraphic Architecture

The general stratigraphic succession within Devereaux Slough follows what is to be expected from a rise in sea levels through the late Pleistocene and Holocene. As sea level rose through the late Pleistocene and Holocene, the coastline moved further inland and the environment at the current location of the slough changed from a fluvial flood plain environment to a slough environment similar to what is observed today. Initial inundation of the fluvial flood plain occurred about 8.5 ka and Devereux Slough alternated between periods of more alluvial fans/fan deltas and more open quiet-water settings. The earlier part of the record is marked by more alluvial fan/fan-delta deposits with a minimum in their occurrence between ~5 ka and 3 ka. This minimum also corresponds to the highest abundance of ostracods and the only occurrence of marine washover deposits (well-sorted sand facies) in the central portions of the lagoon. The more saline-tolerant Sarscypridopsis peaks in abundance around 3ka and decreases in occurrence until the present day (Figures 6 and 7). The larger percentage of Limnocytheridae and Cyprideis in the lower and upper sections of the cores indicate that the environmental conditions were less marine-influenced immediately prior to and after 3 ka. The peak at 3 ka may represent the maximum transgression of the shoreline with a regression to the present day as seen in most continuously submerged coastlines across the globe (Stanley and Warne, 1994; Livsey and Simms, 2016). The peak in salinity may have also been enhanced by the flooding frequency experienced by the lagoon (discussed later).

Storms

The only evidence of marine inundation or overwash within Devereux Slough is the appearance of beds of well sorted sand facies at a depth of 500 cm with a thickness of 35 cm in UDX 15-01 and at a depth of 350 cm in core DX 11-04 with a thickness of over 200 cm. The bottom 10 cm (605 – 615 cm) of core DX 11-04 also contained the well sorted sand facies, which may continue with depth in that location. The maximum age of the sand bed(s) in both cores is constrained by ages obtained from muddy deposits below each sand. In core UDX15-01 a *Cerithidea californica* was dated to 3930 ±410 cal BP 1 cm below the sand contact. Two hundred meters seaward, in core DX11-04, a *Cerithidea californica* shell was dated to 3870 ±410 cal BP 2 cm below the sand contact. The sand beds contain no discernible bedding planes or sedimentary structures, although they may have been destroyed as part of the coring process. In addition, no apparent boundaries or significant changes in magnetic susceptibility are found within the sand beds. The bed in core UDX15-01 shows a weak fining upward trend from an average grain size (D50) of 0.167 mm at it base to 0.137 mm at its top. The sand is subrounded and dominantly composed of quartz (91%), with a few lithic (4%) and feldspar (5%) grains. Less than 5% of the sand grains appear to be frosted, and about 8% are rounded. The sand also contains tar balls. These hydrocarbons may be sourced from the seeps offshore of Coal Oil Point. We cannot determine whether the bed(s) were deposited as a single event or a period of increased washover although an age of 3670 ±60 cal BP 150 cm above the contact in core UDX15-01 suggest the sand bed in that location was deposited in less than 250 years and thus likely a single event. The sand bed in core DX11-04 was deposited between 3870±410 cal BP and 1990 ±70 cal BP, thus sand preserved at this location entered the system over a period of no

more than 1920 years and may represent multiple washover events, but no evidence of continued washover is found after ~2 ka. Potentially, the sandy bed(s) started with a large storm that breached the barrier and reached a maximum inland location between core UDX15-01 and core UDX15-02 (it is absent in the latter core). Washover continued until sometime prior to 1990 cal BP but never reached as far inland as the initial event. The presence of sand in the base of core DX11-04 suggests that washover may have been common earlier in the history of the lagoon as well but did not reach as far inland as core UDX15-01.

The central California coastline was not always lined with beautiful beaches as it is today (Masters 2006). Holocene sand beaches did not appear until 6-7 ka when the rate of sea-level rise slowed and bluff erosion and streams of the transverse ranges had supplied enough sediment to the once rocky coast to build a significant beach system (Masters 2006, Reynolds and Simms 2015). The absence of Pismo clams from Native American middens from 5-4 ka, 3-2 ka and 1 ka is thought to reflect higher frequencies of strong El Niño storms removing the sand from the beaches. El Niño years bring larger waves, more rain and an abundance of energy to the coast. The well sorted sand facies in Devereux Slough occurs between 3.9 ka and 3.6 ka, during a quieter period between heightened El Niño events recorded by Masters (2006), and may suggest that the beaches had enough sand to be carried into the lagoon at that time as described by Masters (2006).

Tsunami

Not only is the California coast susceptible to strong storms including atmospheric river events (Reynolds et al., in review) and strong El Niño winters (Masters, 2006), but

possibly tsunamis as well (Ryan et al 2015, Rockwell et al 2016). Four major uplift events (M >7) are proposed to have occurred at Pitas Point in the Santa Barbara channel within the last 10 ka (Rockwell et al 2016). These events occurred at 955 cal BP, 2090 cal BP, 4400 cal BP and 6670 cal BP. With a nearly complete sedimentary section of this time period recorded within the sediment at Devereux slough we might expect to see evidence of a tsunami if they occurred and reached this part of the coastline. However, no evidence of marine inundation at the times of these proposed earthquakes were found (Fig. 11) and the slough appears to have been a rather stable environment for the past 8.5 ka. The only environmental changes observed are the changes from the bioturbated mud and laminated silts to the brown silt and the inter-fingering of the well sorted sand with the muds and silts discussed above. However, the well-sorted sands were not deposited at the same time as the proposed earthquakes, but occur between 470 and 530 years outside of the time proposed for these events. The one exception is the event at 4.4 ka, which, although the central ages of the events differ by five hundred years, does technically overlap within error (2 sigma but not 1 sigma). These ages were obtained from material within the Bioturbated Mud facies 1cm below the sand, providing a maximum age and thus farther in time from the 4.4 ka event. However, no marine washover beds are recorded at the time of the other 3 events. The absence of evidence for marine washover at the time of the proposed earthquakes suggests that if the earthquake events occurred, they either did not produce a tsunami, the tsunami were limited to the eastern Santa Barbara Channel, or were smaller than the elevation of the barrier separating Devereux slough from the open channel – approximately 2 m.

Laminated Silt Facies and Terrestrial Flooding

The laminated silt facies represents the progradation of alluvial fans/fan deltas into the lagoon from side-feeding gully systems (Fig. 9). Bedsets of this facies correlate across the lagoon and down the axis of the system. If the alternations in the laminated silt facies and bioturbated mud facies represented lobe-avulsions, the bedsets would not be expected to correlate throughout the lagoon. Thus, they provide a potential record of enhanced terrestrial flooding from precipitation runoff. Their distribution in time suggests flooding was more prevalent along the Santa Barbara Channel from 0.9 ka to 2.8 ka , 4.7 ka to 5.2 ka, 6.4 ka to 6.6 ka, 7.2 ka to 7.6 ka and 7.8 ka to 8.6 ka. With the exception of one 20 cm thick bed at a depth of 350 cm, a notable break in storm frequency was observed between 3 ka and 5 ka. The record of fluvial runoff and flooding has the same pattern as periods of higher frequency flood layers within the Santa Barbara Basin (Du et al., 2017), but may lag behind the Santa Barbara Basin record by about 500 years (Fig. 12). The 500 year difference between the Santa Barbara Basin record and that from Devereux Slough may reflect an innacurate radiocarbon reservior (likley in Devereux Slough. But potentially within the Santa Barbara Basin Record). Alternativley it may be a reflection of our age model that does not account for periods of rapid sedimentation that may have occurred during the periods of enhanced terrestial runoff into the lagoon. The similarity in the Devereux Slough and Santa Barbara Basin suggests that the flood layers not only reflect flooding of the major rivers, e.g. Santa Clara and Ventura Rivers, entering the Santa Barbara Basin, but also the smaller gullies and streams along the northern Santa Barbara Channel.

Subsidence

The intertidal gastrapod *C. californica* lives within a well-defined relationship with respect to tidal datums (Simms et al., 2016; Reynolds et al., in review). Two *C. californica* were dated from depths of 539 cm and 567 cm in cores UDX 15-01 and DX 11-04. The core tops are found at elevations of 2.97±0.2 m and 2.19±0.2 m, providing sea-level index points of -2.42±0.2 m at 3930±410 cal BP and -3.48±0.2 m at 3870±410 cal BP, respectively. A comparison between their elevations (E) with that of the time-equivalent elevations of the relative sea-level record (RSL) of Reynolds and Simms (2015) using the following equation:

$$V = (RSL - E) \qquad (1)$$

provides an estimate of the amount of vertical motion (V) experienced at those locations within the slough (Simms et al., 2016). Dividing by the age of the *C. californica*, t, provides a rate of vertical motion (Rv) via the following expression:

$$Rv = (V/t) \qquad (2)$$

The errors in the magnitude of vertical motion (δ_v) were determined using the following equation:

$$\delta_v = (\delta_{RSL}^2 + \delta_E^2)^{0.5} \qquad (3)$$

where δ_{RSL} and δ_E are the errors in the relative sea-level record of Reynolds and Simms (2015)(±1.5 m) and the elevation of the index points, respectively. The error in the rate of vertical motion (δ_{rv}) was determined by combining the errors using the following equation:

$$\delta_{rv}/Rv = ((\delta_v/V)^2 + (\delta_t/t)^2)^{0.5} \qquad (4)$$

Following equation (2) the slough is uplifting at a rate of 0.05±0.39 mm/yr in core UDX15-01 and subsiding at a rate of 0.23±0.39 mm/yr in core DX 11-04 (Table 2). These two values fall within error of zero. Accounting for subsidence would make each of those

values more positive (uplift) suggesting that the South branch of the Moore Ranch Fault is located north of cores UDX15-01 and DX11-04.

Conclusions

Six sediment cores from Devereux Slough contain five facies, a Pebbly Sandy Mud from the construction of the golf course, a bioturbated mud representing a shallow lagoon, laminated silts representing small alluvial fans, a well sorted sand representing overwash deposits, and a brown silt representing an alluvial or fluvial floodplain. No evidence of marine washover were found at the time of reported large earthquakes on the Pitas-Point Thrust suggesting that either the earthquakes were not tsunamigenic, tsunami only occurred farther to the east, or the tsunami were less than 2 m in height. Only one possible marine-sourced event bed was observed at 3.9 ka within the ~16 ka record and is interpreted to represent a storm marking the beginning of a period of heightened long shore transport along the coast when the frequency of storms was subdued. The laminated silts represent periods of runoff from fluvial-sourced flooding with peaks at 2.0 ka, 5.1 ka, 6.5 ka, 7.5 ka, 8.5 ka and a lull in flooding between 5 ka and 3 ka. The elevation of two *Cerithidea californica* suggest the north portion of the slough is uplifting at a rate of 0.05±0.39 mm/yr while the southern portion of the slough is subsiding at a rate of 0.23±0.39. As both are within error of zero subsidence, the More Ranch Fault is likely located north of the two cores.

Tables

Radiocarbon ages

Lab code	Core	Sample type	Depth (cm)	Raw 14C age (yrs BP)	Calendar ages (cal years BP)	Calendar 2σ age range (cal yrs BP)
UCIAMS-169335	UDX15-01	organic	230	1030±15	940	930-960
UCIAMS-169338	UDX15-01	organic	403	3420±25	3670	3590-3720
UCIAMS-169333	UDX15-01	C. californica	539	4105±15	3930	3540-4370
UCIAMS-169337	UDX15-01	organic	684	4257±20	4840	4830-4860
UCIAMS-169329	UDX15-01	organic	779	5580±20	6360	6310-6400
UCIAMS-169325	UDX15-01	organic	912	5555±30	4350	6300-6400
UCIAMS-169327	UDX15-01	organic	1013	6470±25	7340	7320-7400
UCIAMS-169328	UDX15-01	organic	1115	7075±25	7900	7850-7910
UCIAMS-169331	UDX15-01	organic	1228	6535±25	7450	7420-7490
UCIAMS-169330	UDX15-01	organic	1280	6955±45	7790	7680-7870
UCIAMS-183707	UDX15-01	organic	1583	15220±60	18490	18330-18650
UCIAMS-183709	UDX15-02	organic	224	170±15	190	170-220
UCIAMS-183691	UDX15-02	bivalve	505	4015±15	3750	3416-4087
UCIAMS-183711	UDX15-02	organic	782	5575±20	6360	6310-6400
UCIAMS-183712	DX11-03	organic	34	260±20	300	280-320
UCIAMS-183713	DX11-03	organic	138	1895±15	1850	1820-1880
UCIAMS-183714	DX11-03	organic	155	2025±20	1970	1920-2010
UCIAMS-191125	DX11-04	organic	35	750±60	700	630-790
UCIAMS-191126	DX11-04	organic	52	1100±280	1040	550-1550
UCIAMS-191123	DX11-04	organic	326	2030±25	1980	1920-2060
UCIAMS-191137	DX11-04	C. californica	567	4060±25	3860	3460-4290

Table 1: Radiocarbon ages collected as part of this study. Calib 7.1 was used to calibrate all ages with a reservoir age of 171±154 used for the two *C. californica* samples and 217±129 was used for one bivalve sample (Holmquist et al., 2015).

Subsidence Calculations

Core	RSL (m)	δ_{RSL} (m)	E (m)	δ_E (m)	V (m)	Rv (m/yr)	δ_v (m)	δ_{rv}/Rv (m/yr)	Rate (mm/yr)
UDX15-01	2.6	1.5	-2.42	0.2	-0.18	-4.6×10^{-5}	1.5	8.4	-0.05±0.39
DX11-04	2.6	1.5	-3.48	0.2	0.88	2.3×10^{-4}	1.5	1.7	0.23±0.39

Table 2: Calculations used to determine rates of vertical motion from the two C. californica samples in cores UDX15-01 and DX11-04.

Figures

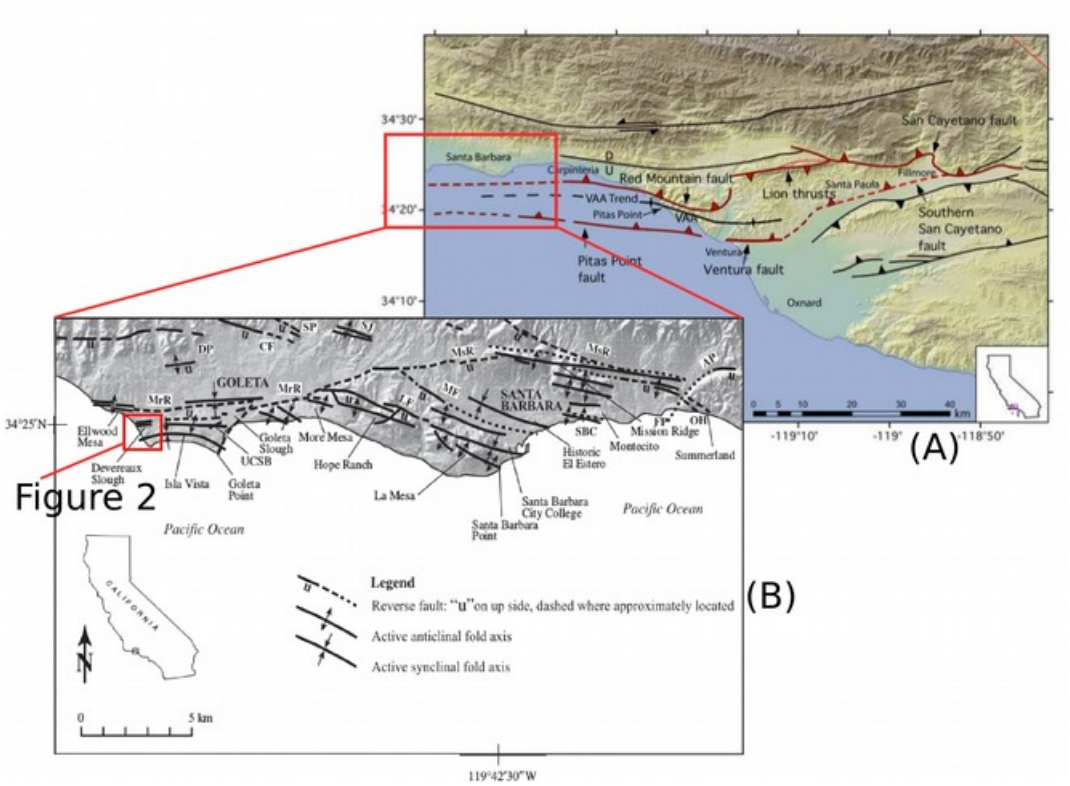

Figure 1: (A) Regional overview, color map from Rockwell et al (2016) showing the location of the Ventura-Pitas Point Thrust within the western Transverse Ranges. The area of figure 2 is indicated by the red box, and the VAA Trend is the Ventura Avenue anticlinal trend offshore.(B) Hillshade map from Gurrola et al (2014) showing the location of the major geological structures in the greater Santa Barbara area including the Mission Ridge fault system, which is subdivided into the More Ranch (MrR), the Mission Ridge (MsR), and the Arroyo Parida (AP) segments, and several reverse faults including the Dos Pueblos (DP), the Carneros (CF), the San Jose (SJ), the San Pedro (SP), the Lavigia (LF), the Mesa (MF), the Santa Barbara Cemetery (SBC), the Ortega Hill (OH), and the Fernald Point (FP) faults. UCSB refers to the University of California–Santa Barbara. The area of figure 2 is indicated by the red box, and the VAA Trend is the Ventura Avenue anticlinal trend offshore.

Figure 2: Location of cores collected in Devereux Slough and the approximate location of the local Moore Ranch Fault based on the work of Gurrola et al (2014). See Figure 1 for general location.

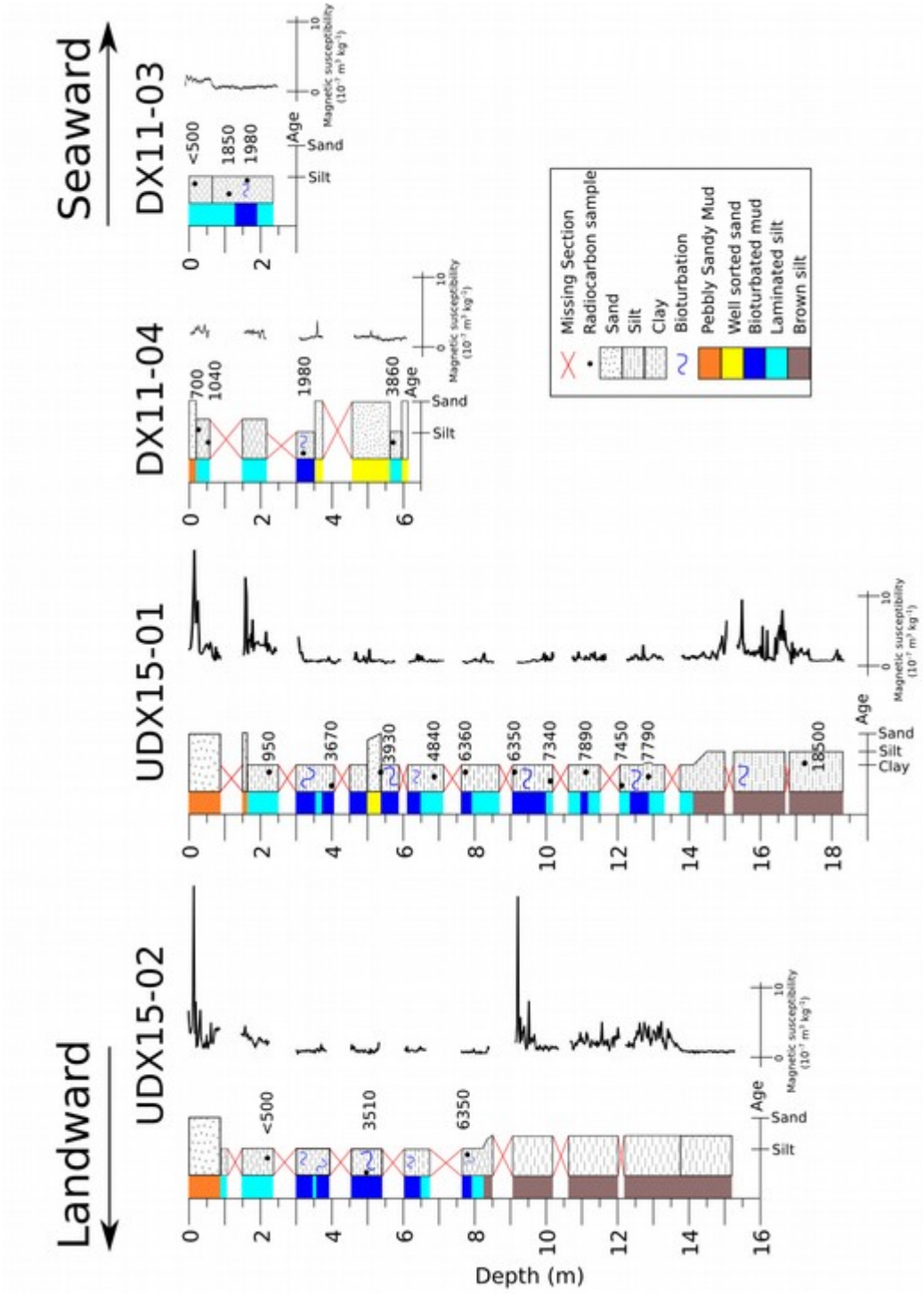

Figure 3: Dip-oriented profile of core descriptions collected in Devereux Slough. See Figure 2 for core locations. Landward is to the northwest and seaward is to the south.

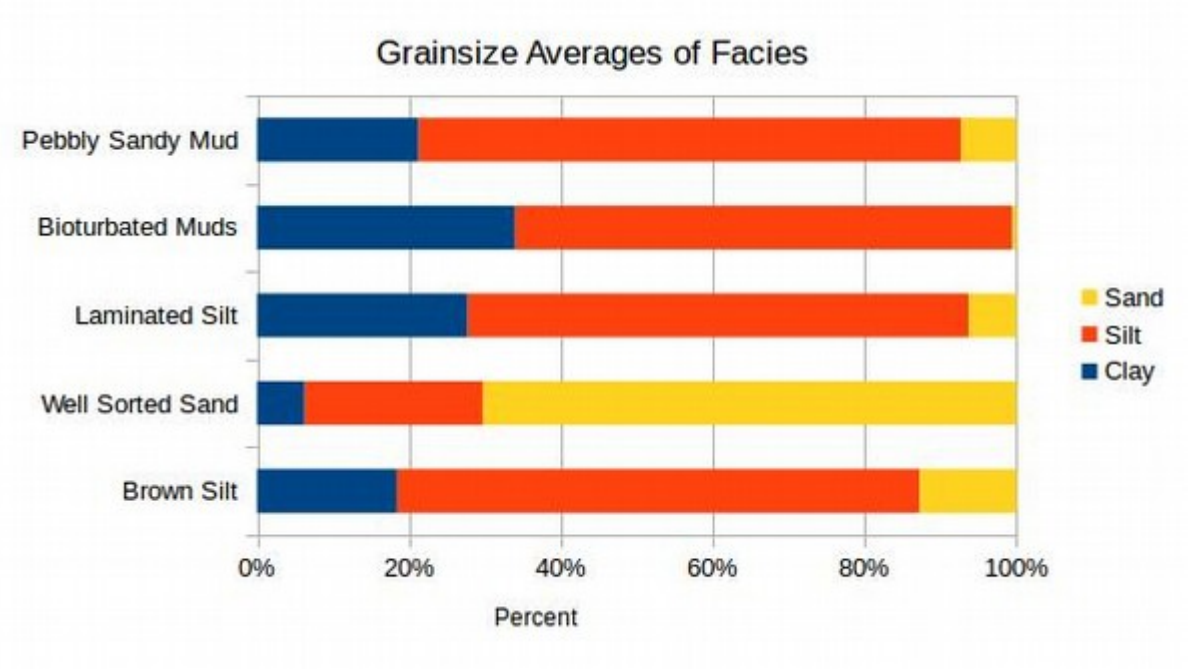

Figure 4: Average sand, silt, and clay contents for the facies defined in this study.

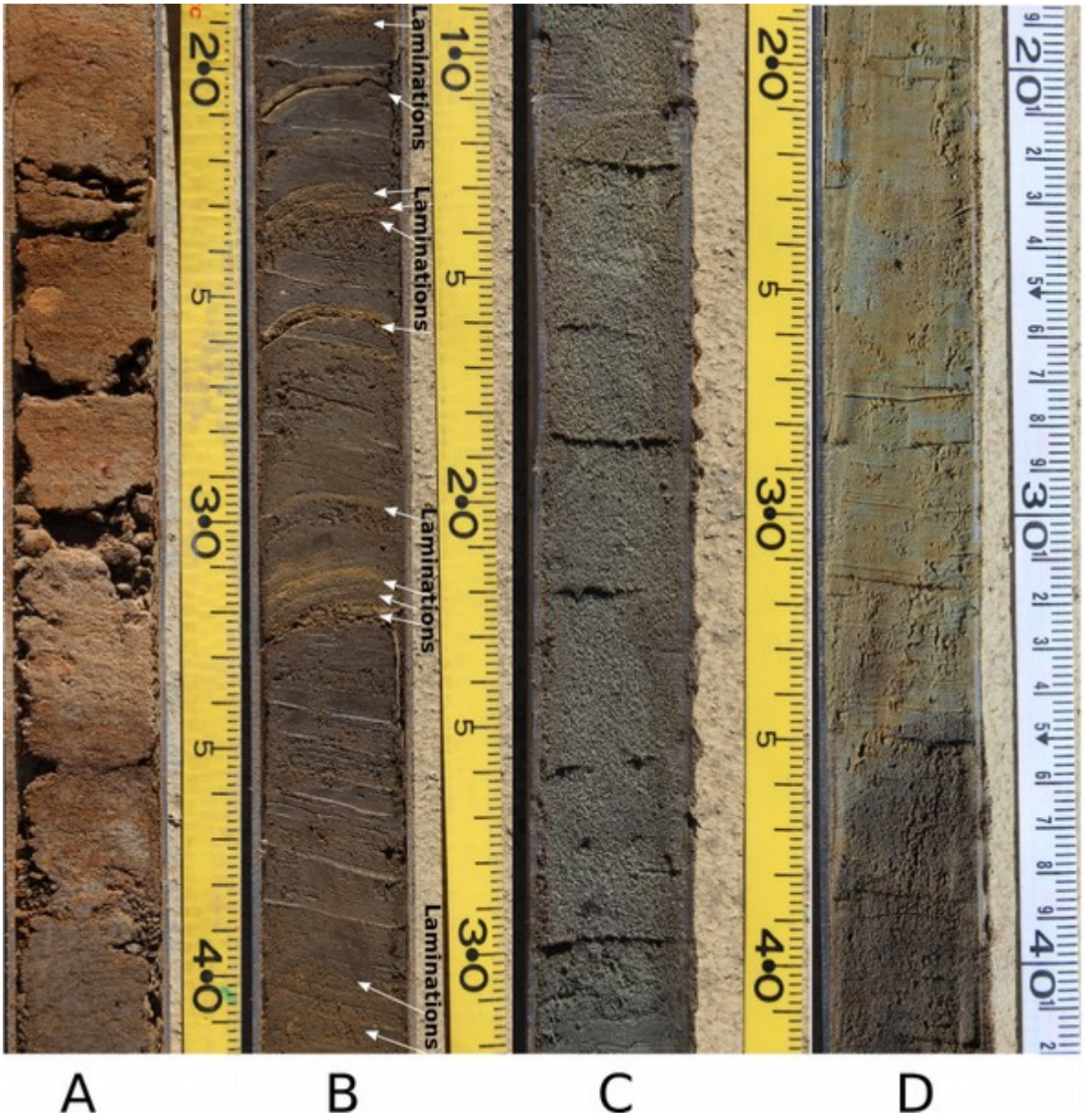

Figure 5: Pictures of core UDX15-01 showing the Pebbly Sandy Mud at depths of 20-40 cm (A), Laminated Silts at depths of 210-230 cm with large laminations highlighted (B), Well Sorted Sand Facies at depths of 520-540 cm (C), Bioturbated Muds at depths of 620-630 cm (D top) and Brown Silt Facies from a depth of 630-640 cm (D bottom). See Figure 3 for complete core descriptions.

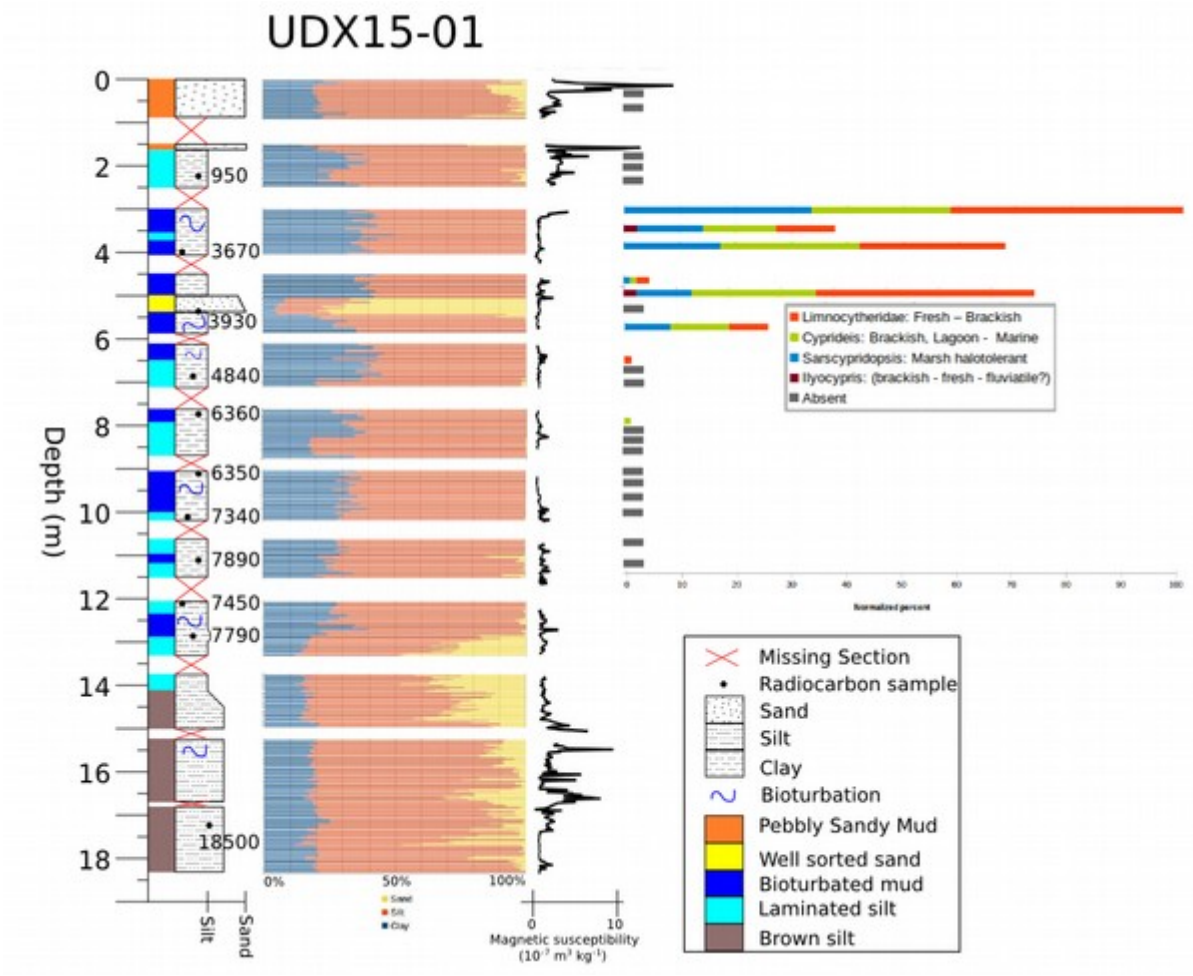

Figure 6: Description of core UDX 15-01 including grainsize, facies classification, magnetic susceptibility, ages and ostracod abundances. See Figure 2 for core location.

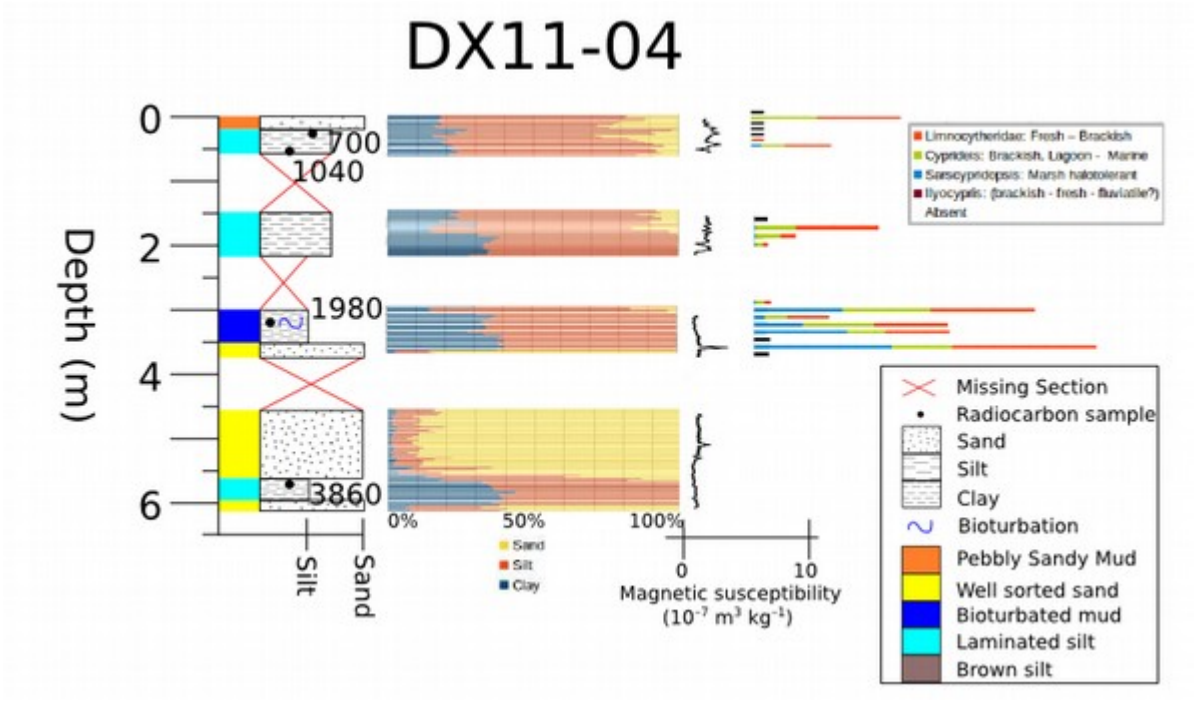

Figure 7: Description of core DX 11-04 including, grain size, facies classification, magnetic susceptibility, ages and ostracod abundances. See Figure 2 for core location.

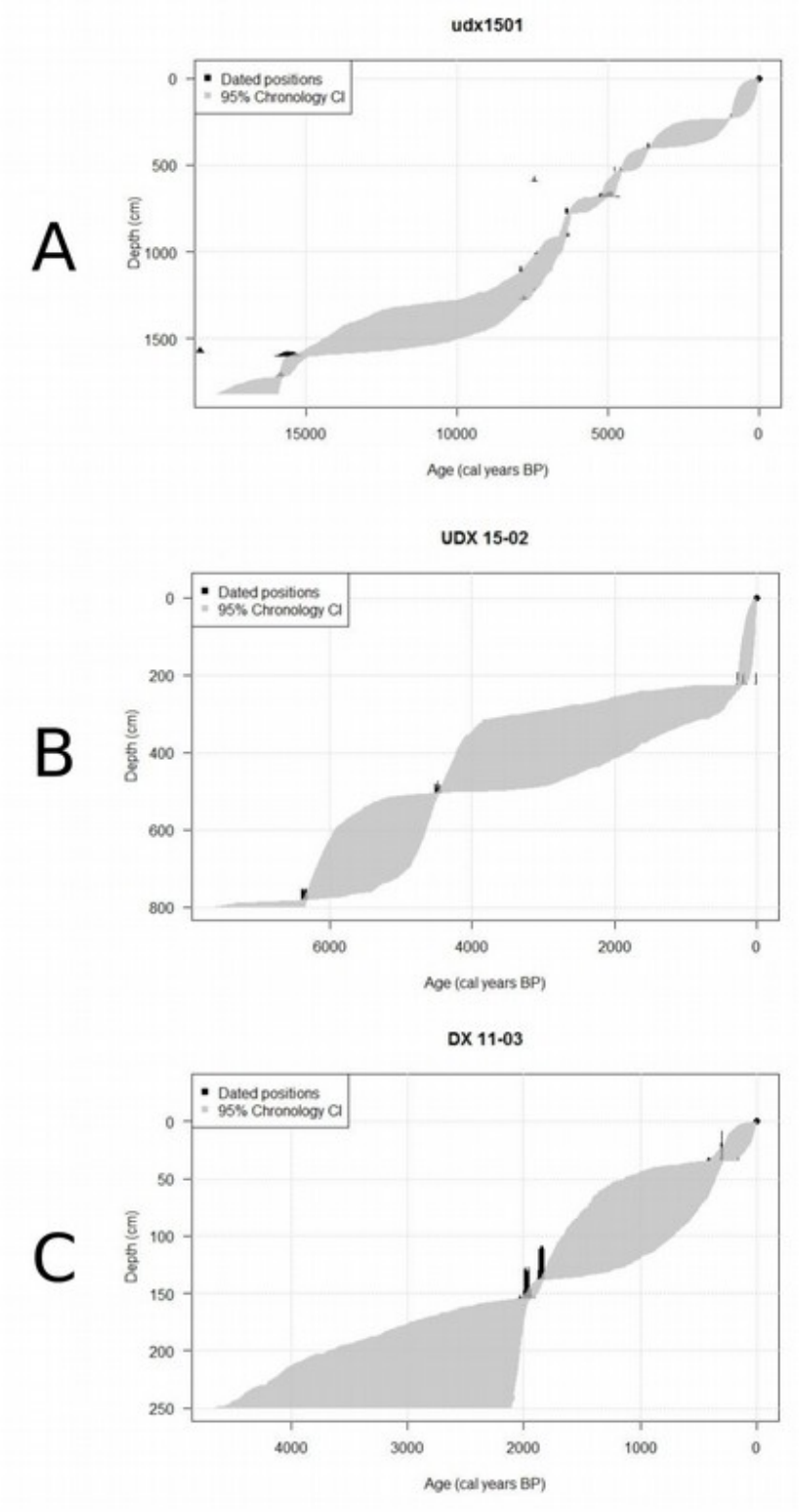

Figure 8: Bchron plot from cores (A) UDX 15-01, (B) UDX15-02 and (C) DX 11-03. See Figure 2 for core locations and Table 1 for the radiocarbon ages used for the plots.

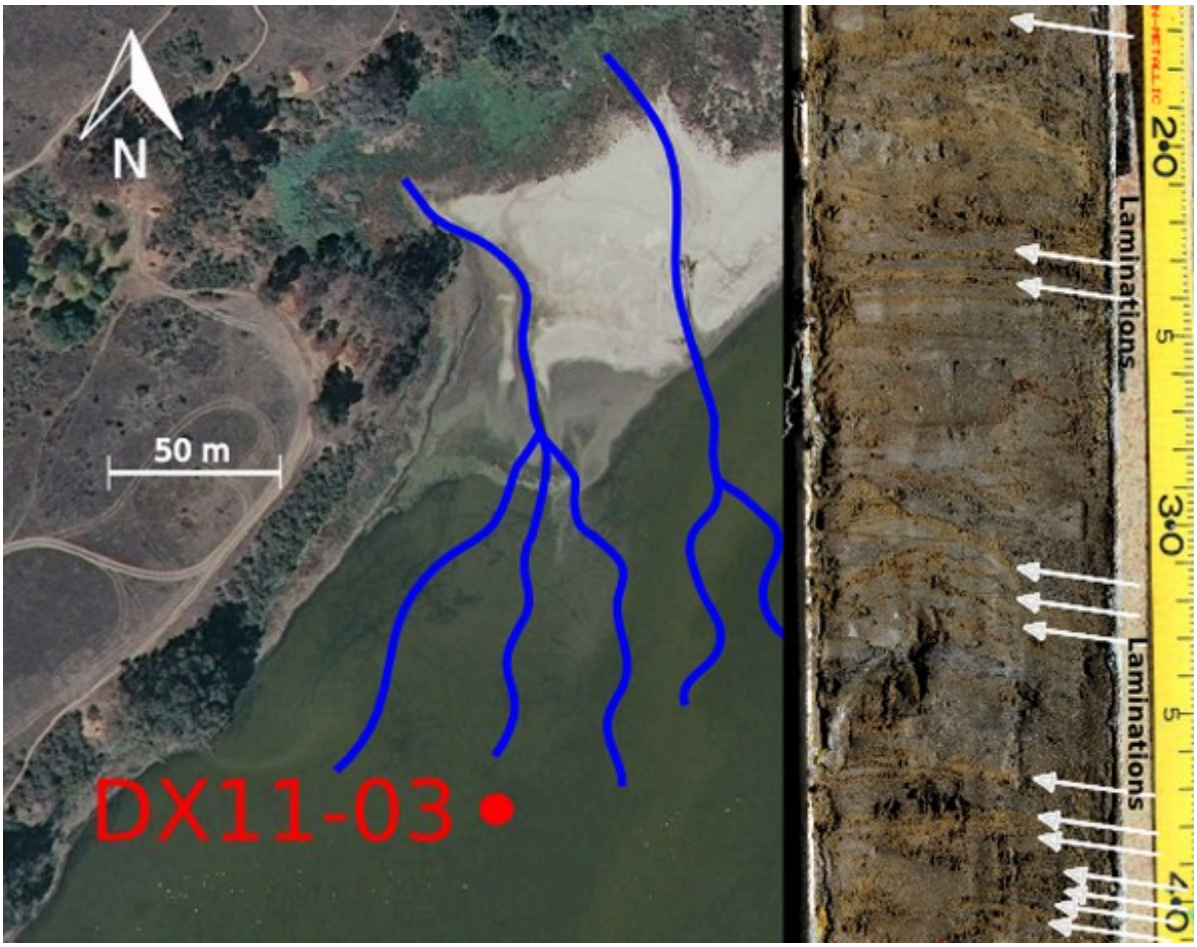

Figure 9: Google image of Devereux Slough and photograph of 17 cm to 41 cm within core DX11-03. Note the alluvial fans developed where the two gullies enter the slough. The Laminated Silt Facies within the core is thought to represent this depositional environment. Laminations are highlighted, see Figure 2 for general location.

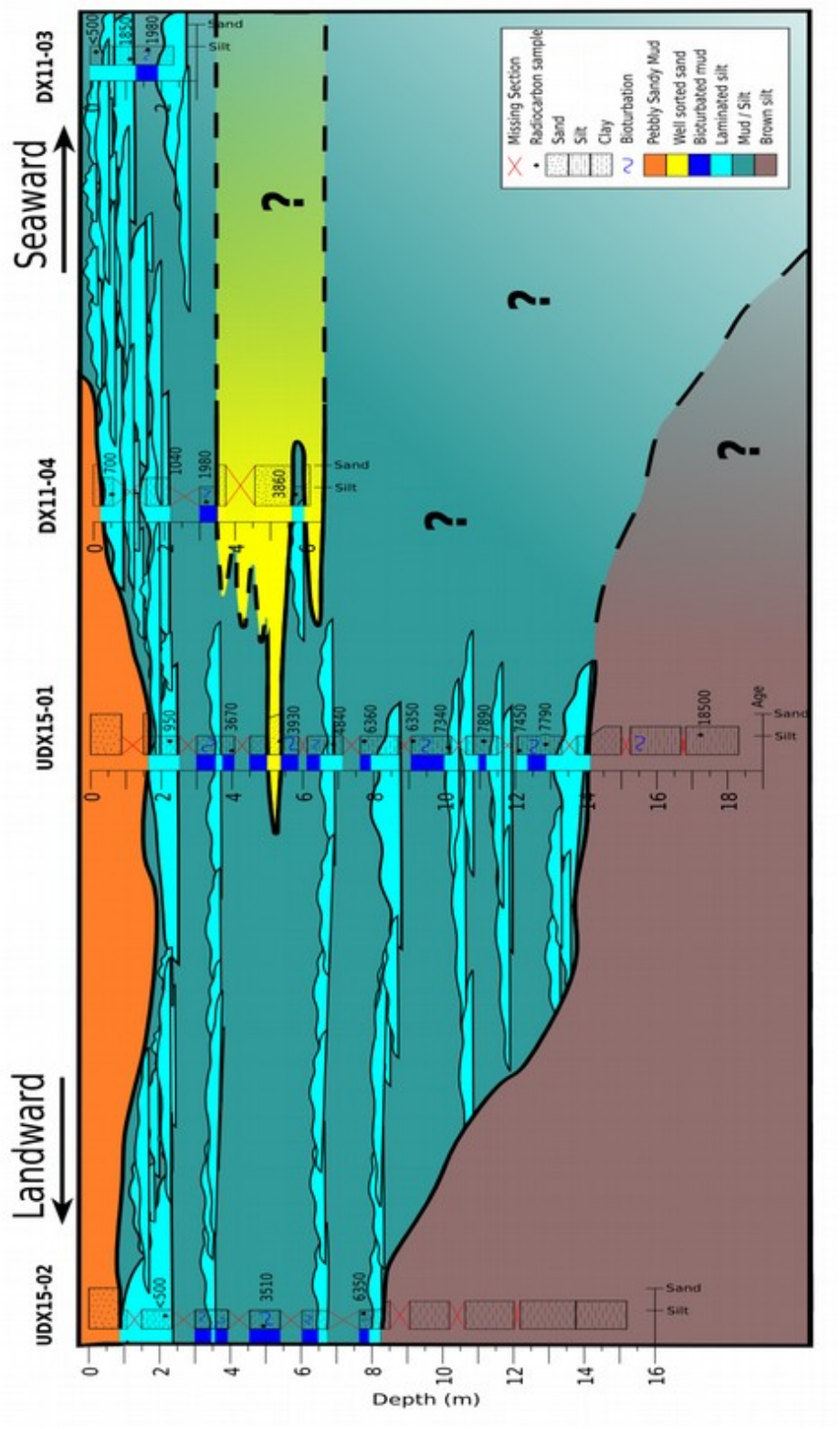

Figure 10: Geologic cross-section through Devereux Slough from the northwest (landward) towards the south (seaward). See Figure 2 for core locations.

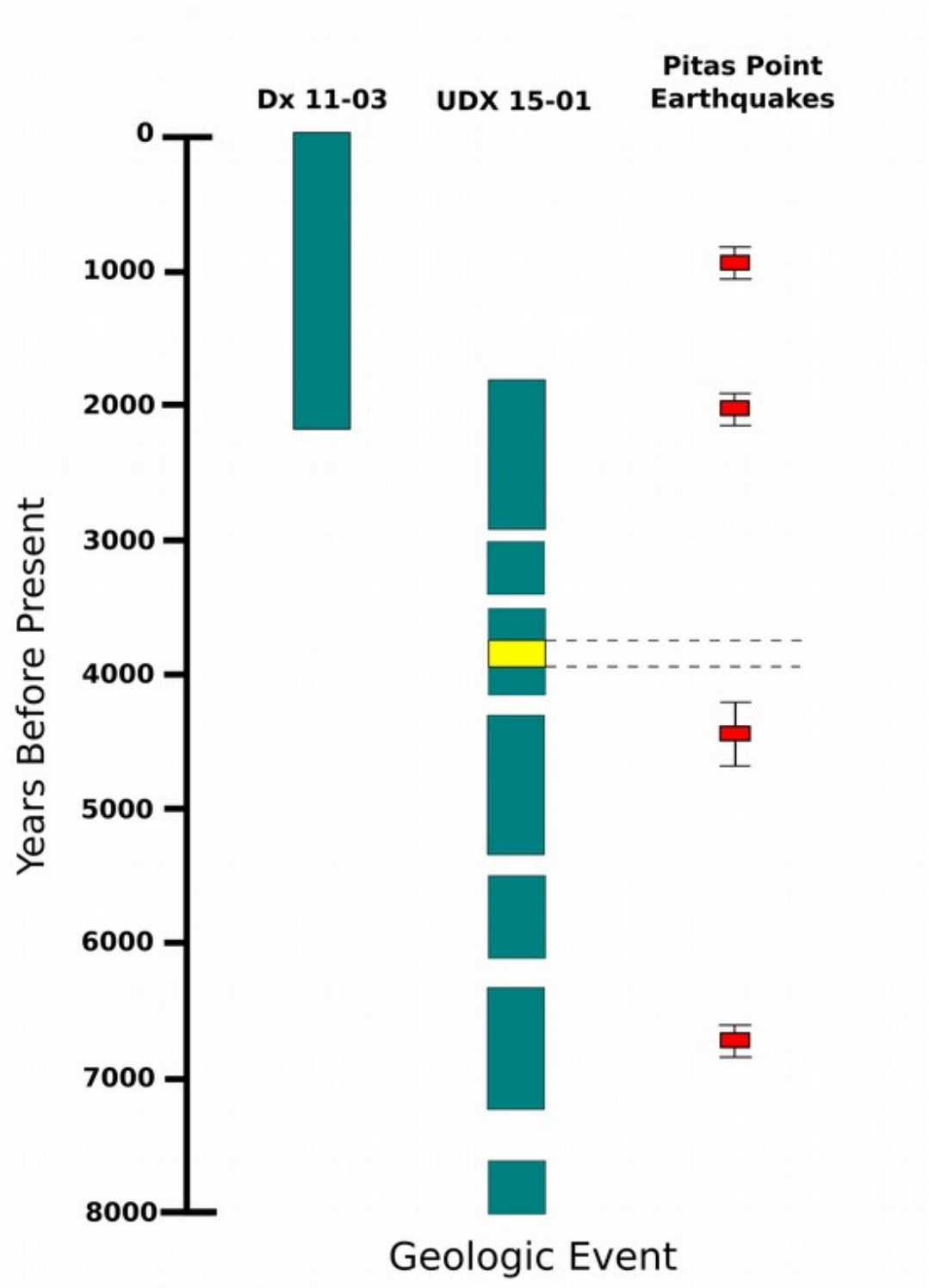

Figure 11: Occurrence of large magnitude earthquakes at Pitas Point (red), temporally aligned with sediment cores. Teal represents fine-grained lagoonal deposits (laminated silt or bioturbated mud facies) and yellow represents marine washover deposits (well-sorted sand facies). See Figure 2 for core locations.

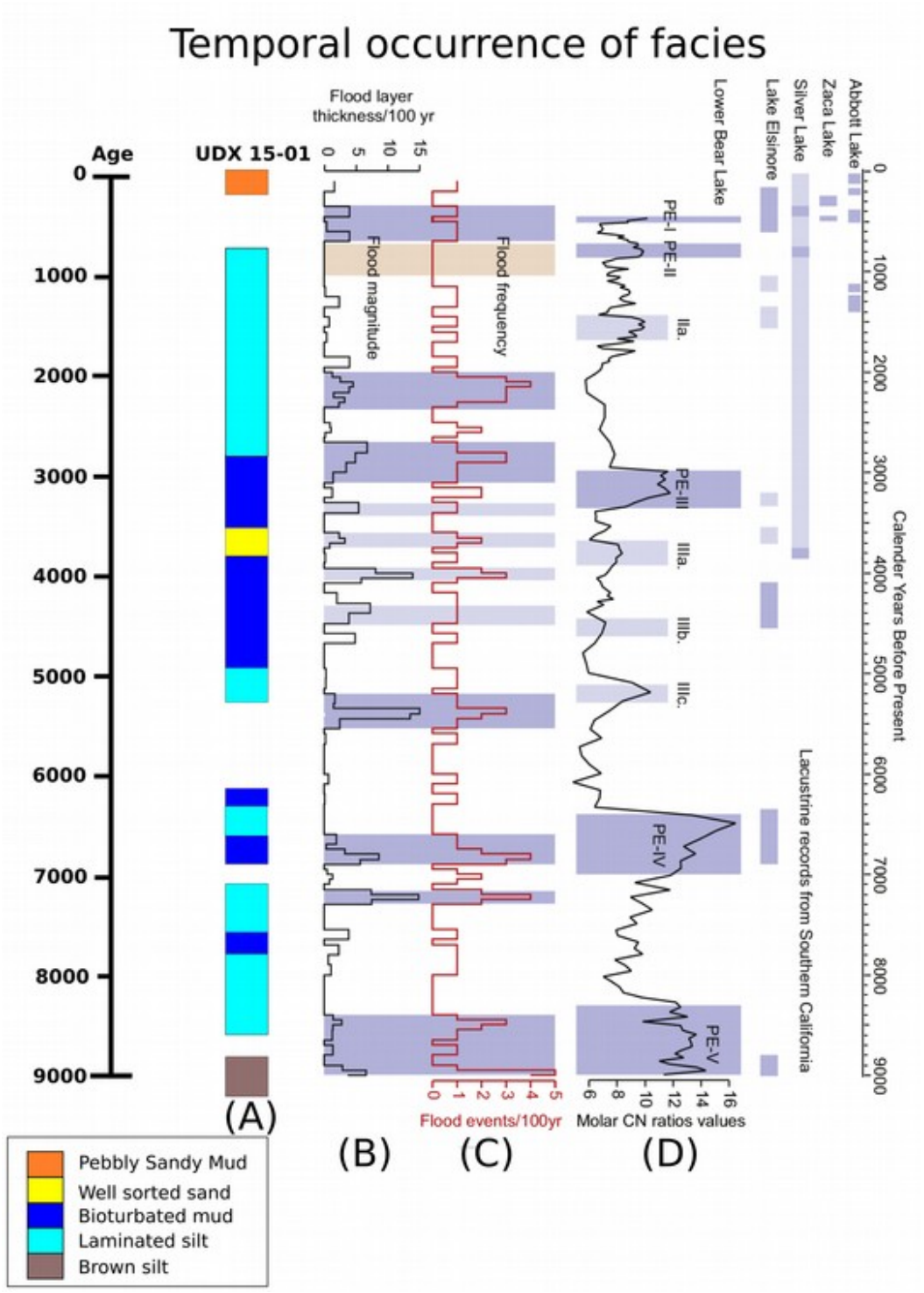

Figure 12: (A) Temporal occurrence of facies in core 15-01 aligned with flood summary from Du et al. 2018 (B) Flood magnitude (flood layer thickness per century), (C) Flood frequency curve (flood events per century), (D) Lacustrine records from Abbott Lake (Hiner et al., 2016), Zaca Lake (Kirby et al., 2014), Silver Lake (Kirby et al., 2015) and Lake Elsinore (Kirby et al., 2010) in Southern California.

References

Bard, E., Hamelin, B. and Arnold, M., 1997. Deglacial sea-level record from Tahiti corals and the timing of global meltwater discharge. Oceanographic Literature Review, 2(44), p.99.

Belknap, D.F. and Kraft, J.C., 1985. Influence of antecedent geology on stratigraphic preservation potential and evolution of Delaware's barrier systems. Marine geology, 63(1-4), pp.235-262.

Cook, E.R., Woodhouse, C.A., Eakin, C.M., Meko, D.M. and Stahle, D.W., 2004. Long-term aridity changes in the western United States. Science, 306(5698), pp.1015-1018.

Dias, K. and Sperazza, M., 2014, October. Statistical evaluation of grain size facies model for barrier island systems, fire island, new york. In 2014 GSA Annual Meeting in Vancouver, British Columbia.

Dibblee, T.W., 1966. *Geology of the Central Santa Ynez Mountains, Santa Barbara County, California* (Vol. 186). California Division of Mines and Geology.

Du, X., Hendy, I. and Schimmelmann, A., 2017. A 9000-year flood history for Southern California: A revised stratigraphy of varved sediments in Santa Barbara Basin. Marine Geology.

Elliott, E.A., McKee, B.A. and Rodriguez, A.B., 2015. The utility of estuarine settling basins for constructing multi-decadal, high-resolution records of sedimentation. *Estuarine, Coastal and Shelf Science*, *164*, pp.105-114.

Fairbanks, R.G., 1989. A 17,000-year glacio-eustatic sea level record: influence of glacial melting rates on the Younger Dryas event and deep-ocean circulation. Nature, 342(6250), pp.637-642.

Gurrola, L.D., Keller, E.A., Chen, J.H., Owen, L.A. and Spencer, J.Q., 2014. Tectonic geomorphology of marine terraces: Santa Barbara fold belt, California. Geological Society of America Bulletin, 126(1-2), pp.219-233.

Haslett, J. and Parnell, A., 2008. A simple monotone process with application to radiocarbon-dated depth chronologies. Journal of the Royal Statistical Society: Series C (Applied Statistics), 57(4), pp.399-418.

Holmquist, J.R., Reynolds, L., Brown, L.N., Southon, J.R., Simms, A.R. and MacDonald, G.M., 2015. Marine radiocarbon reservoir values in southern California estuaries: interspecies, latitudinal, and interannual variability. Radiocarbon, 57(3), pp.449-458.

Hubbard, J., Shaw, J.H., Dolan, J., Pratt, T.L., McAuliffe, L. and Rockwell, T.K., 2014. Structure and seismic hazard of the Ventura Avenue anticline and Ventura fault, California: Prospect for large, multisegment ruptures in the western Transverse Ranges. Bulletin of the Seismological Society of America.

Johnson, Samuel Y., Guy R. Cochrane, Nadine E. Golden, Peter Dartnell, Stephen R. Hartwell, Susan A. Cochran, and Janet T. Watt. "The California Seafloor and Coastal Mapping Program–Providing science and geospatial data for California's State Waters." Ocean & Coastal Management 140 (2017): 88-104.

Kirby, M.E., Lund, S.P., Anderson, M.A. and Bird, B.W., 2007. Insolation forcing of Holocene climate change in Southern California: a sediment study from Lake Elsinore. Journal of Paleolimnology, 38(3), pp.395-417.

Kirby, M.E., Lund, S.P., Patterson, W.P., Anderson, M.A., Bird, B.W., Ivanovici, L., Monarrez, P. and Nielsen, S., 2010. A Holocene record of Pacific decadal oscillation (PDO)-related hydrologic variability in southern California (Lake Elsinore, CA). Journal of Paleolimnology, 44(3), pp.819-839.

Kirby, M.E., Feakins, S.J., Hiner, C.A., Fantozzi, J., Zimmerman, S.R., Dingemans, T. and Mensing, S.A., 2014. Tropical Pacific forcing of Late-Holocene hydrologic variability in the coastal southwest United States. Quaternary Science Reviews, 102, pp.27-38.

Livsey, D. and Simms, A.R., 2016. Episodic flooding of estuarine environments in response to drying climate over the last 6000years in Baffin Bay, Texas. Marine Geology, 381, pp.142-162.

Marshall, S.T., Funning, G.J. and Owen, S.E., 2013. Fault slip rates and interseismic deformation in the western Transverse Ranges, California. Journal of Geophysical Research: Solid Earth, 118(8), pp.4511-4534.

Marshall, S.T., Funning, G.J., Krueger, H.E., Owen, S.E. and Loveless, J.P., 2017. Mechanical models favor a ramp geometry for the Ventura-pitas point fault, California. Geophysical Research Letters, 44(3), pp.1311-1319.

Masters, P.M., 2006. Holocene sand beaches of southern California: ENSO forcing and coastal processes on millennial scales. Palaeogeography, Palaeoclimatology, Palaeoecology, 232(1), pp.73-95.

McAuliffe, L.J., Dolan, J.F., Rhodes, E.J., Hubbard, J., Shaw, J.H. and Pratt, T.L., 2015. Paleoseismologic evidence for large-magnitude (Mw 7.5–8.0) earthquakes on the Ventura blind thrust fault: Implications for multifault ruptures in the Transverse Ranges of southern California. Geosphere, 11(5), pp.1629-1650.

Minor, S.A., Kellogg, K.S., Stanley, R.G., Gurrola, L.D., Keller, E.A. and Brandt, T.R., 2009. Geologic Map of the Santa Barbara Coastal Plain Area, Santa Barbara County, California. US Department of the Interior, US Geological Survey.

Reimer, P.J., Bard, E., Bayliss, A., Beck, J.W., Blackwell, P.G., Ramsey, C.B., Buck, C.E., Cheng, H., Edwards, R.L., Friedrich, M. and Grootes, P.M., 2013. IntCal13 and Marine13 radiocarbon age calibration curves 0–50,000 years cal BP. Radiocarbon, 55(4), pp.1869-1887.

Reynolds, L.C. and Simms, A.R., 2015. Late Quaternary relative sea level in southern California and Monterey Bay. Quaternary Science Reviews,126, pp.57-66.

Rockwell, T.K., Keller, E.A. and Dembroff, G.R., 1988. Quaternary rate of folding of the Ventura Avenue anticline, western Transverse Ranges, southern California. Geological Society of America Bulletin, 100(6), pp.850-858.

Rockwell, T.K., Clark, K., Gamble, L., Oskin, M.E., Haaker, E.C. and Kennedy, G.L., 2016. Large Transverse Range Earthquakes Cause Coastal Upheaval near Ventura, Southern California. Bulletin of the Seismological Society of America, 106(6), pp.2706-2720.

Ryan, K.J., Geist, E.L., Barall, M. and Oglesby, D.D., 2015. Dynamic models of an earthquake and tsunami offshore Ventura, California. Geophysical Research Letters, 42(16), pp.6599-6606.

Simkins, L.M., Simms, A.R., Cruse, A.M., Troiani, T., Atekwana, E.A., Puckette, J. and Yokoyama, Y., 2012. Correlation of early and mid-Holocene events using magnetic susceptibility in estuarine cores from bays along the northwestern Gulf of Mexico. Palaeogeography, Palaeoclimatology, Palaeoecology, 346, pp.95-107.

Simms, A., Reynolds, L.C., Bentz, M., Roman, A., Rockwell, T. and Peters, R., 2016. Tectonic subsidence of California estuaries increases forecasts of relative sea-level rise. Estuaries and coasts, 39(6), pp.1571-1581.

Stanley, D.J. and Warne, A.G., 1994. Worldwide initiation of Holocene marine deltas by deceleration of sea-level rise. Science-New York then Washington-, pp.228-228.

University of California Santa Barbara Environmental Impact Report for Faculty and Family Student Housing, open space plan and LRDP amendment 2004.

Warrick, J.A., Melack, J.M. and Goodridge, B.M., 2015. Sediment yields from small, steep coastal watersheds of California. Journal of Hydrology: Regional Studies, 4, pp.516-534.

Appendix

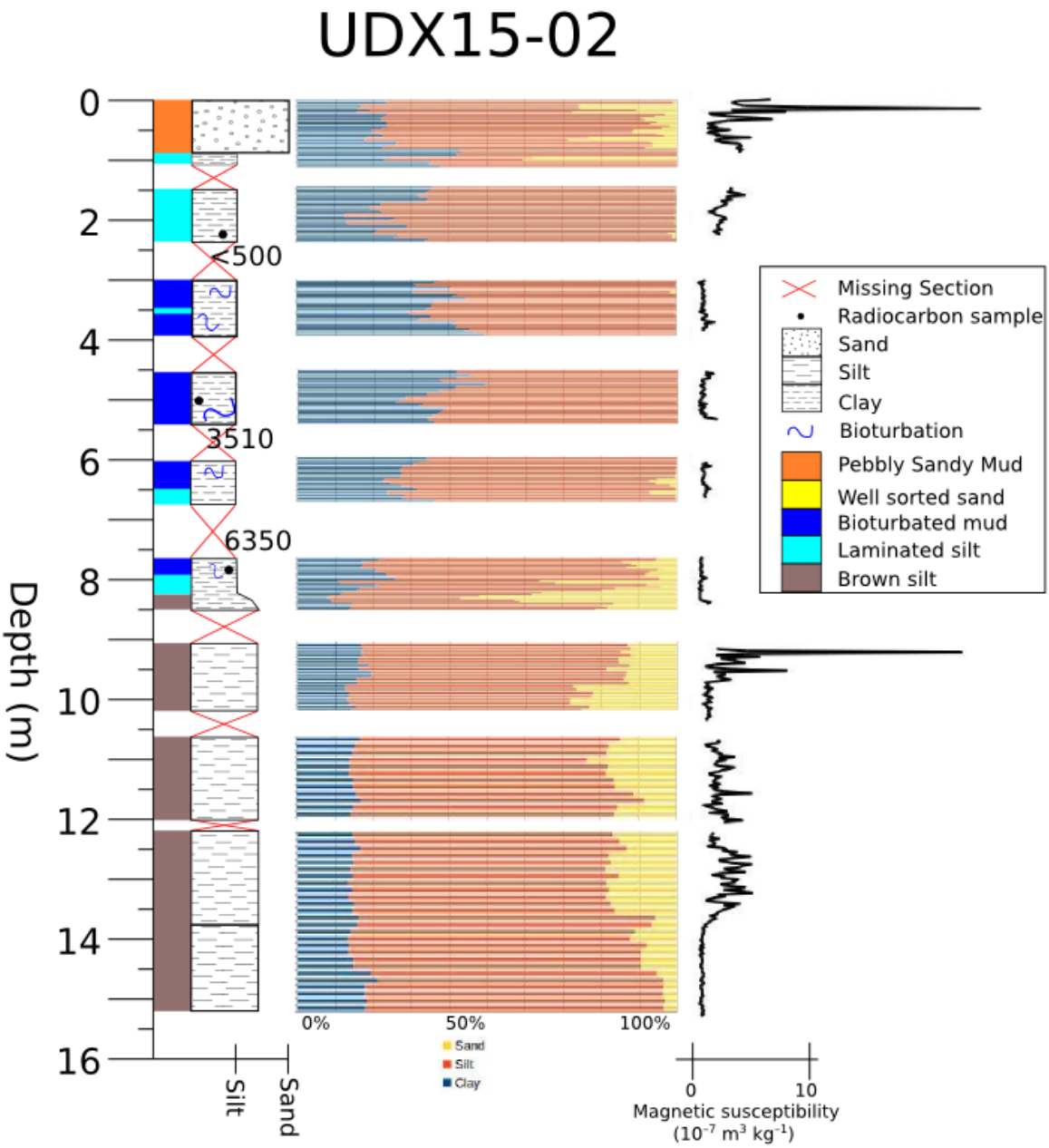

Figure A1: Description of core UDX 15-02 including grainsize, facies classification, magnetic susceptibility, and ages. See Figure 2 for core location.

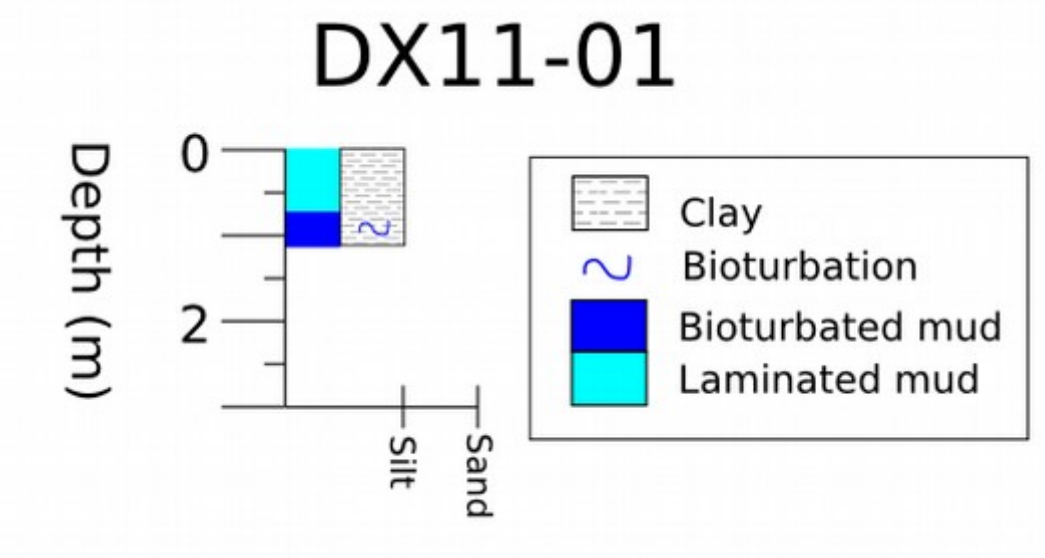

Figure A2: Core log of DX11-01 with facies classification.

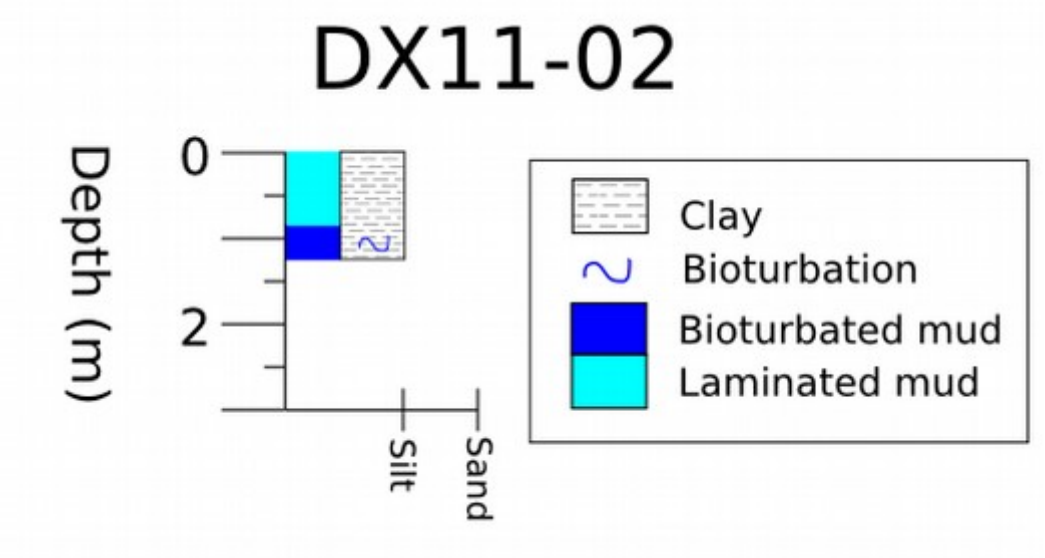

Figure A3: Core log of DX11-02 with facies classification.